Applications of a high-stability scanning tunneling microscope

by H. van Kempen
G. F. A. van de Walle

We have constructed a scanning tunneling microscope which is quite insensitive to vibrations and has a low thermal drift. Low thermal drift is obtained by using a compensating structure for the *z*-axis (perpendicular to the sample surface) of the scan unit and by utilizing symmetry in the *x*- and *y*-directions. To get a low sensitivity to vibrations, we made the scanning unit compact and rigid. A very light tip holder construction allows a high scan speed. We studied different surfaces of Ag single crystals and compared the results with a study of the same surfaces from the inside by a method based on the use of focused conduction electrons. A terrace surface model, introduced to explain the focusing results, has been confirmed for the Ag(001) surface. A description of tip preparation and tip shape is given.

Introduction

To the large number of surface study methods available to the surface scientist a new, very powerful, tool has recently been added [1]: the scanning tunneling microscope method (STM). This new method has in common with most other surface study techniques that the surface is studied from the outside. In this paper we describe how STM can be used to complement another technique, transverse electron focusing (TEF), which studies the surface from the inside. This last method, invented by Tsoi [2], is based on manipulation of conduction electrons and gives information on the interaction of those electrons with the sample surface and interfaces.

In the first part of this paper a description of our STM is given. The second part describes how the STM can be used to find the answer to a question coming from the TEF field. In the last part of the paper some aspects of the tip preparation and tip shape are described.

1. STM construction

Construction of the scanning tunneling microscope was aimed at attaining the following objectives: low thermal drift, insensitivity to vibrations, and high scanning speed. Our STM consists of a stepping system ("louse") on which the sample is mounted and a continuous system which carries the tip. In the continuous system the thermal drift was diminished by two methods: symmetry and compensation. In the *x*-*y* directions (lateral directions) we used a symmetric arrangement of piezoelectric and stainless-steel cubes, as shown in **Figure 1**. The center cube, to which the tip is connected via *z*-direction piezoelectric elements, is moved by activating rows of *x*- and *y*-piezoelectric cubes (*E*-field in *z*-direction). Because of this symmetric configuration thermal drift is diminished.

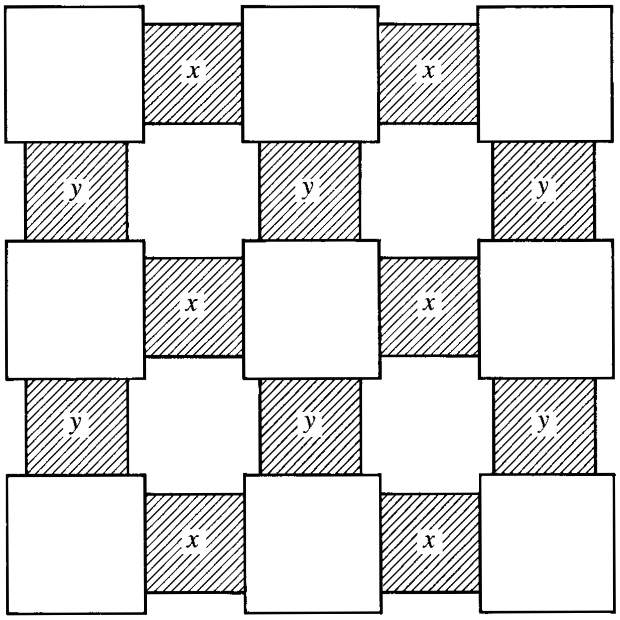

Figure 1

Continuous x-y-displacement system. Shaded squares indicate x- and y-piezoelectric cubes, while unshaded squares indicate stainless-steel cubes. The tip holder is mounted via the Z_1-piezoelectric system (see Figure 2) on the central cube. The cubes at the corners are connected to the base plate via the Z_2-piezoelectric system.

In the z-direction a compensating structure, as shown in **Figure 2**, is used. There are two sets of z-piezoelectric elements, Z_1 and Z_2. Z_2 moves the total x-y assembly, while Z_1 moves only the very light tip holder and tip. To get a simple electrical configuration both Z_1 and Z_2 are built up from pairs of piezoelectric cubes. In this way the stainless-steel cubes at the corners and the base plate can be at ground potential.

To get a low sensitivity for external vibrations, we tried to make the construction compact and rigid, with internal resonance frequencies as high as possible. Consequently the x-y range is quite limited. Using the maximum voltages allowed for the x-y cubes the scanning limits are 8000×8000 Å^2. However, for practical reasons (voltage limit of UHV feedthrough, etc.) we were limited to 3000×3000 Å^2. This x-y deflection is about two times larger than expected from the electromechanical coefficient of the piezoelectric material. This is probably due to the constraints exerted on the x- (respectively y-) piezoelectric cubes by the neighboring stainless-steel cubes in the y- (respectively x-) direction.

Although in normal operation the Z_2-piezoelectric cubes are not used, the presence of two sets of z-piezoelectric elements is very convenient for evaluating the mechanical and electronic properties of the system. To measure the frequency response of the system in normal operation including the feedback loop, we applied a white-noise voltage across the Z_2-piezoelectric cubes and determined the response function from the correlation between the applied white noise and the feedback signal (**Figure 3**). By opening the feedback loop, applying the white-noise voltage successively to Z_1 and Z_2 and simultaneously observing the tunneling signal, it could be concluded that the peak at 1.5 kHz in Figure 3 is due to a mechanical resonance of the x-y-piezoelectric system. This resonance is (nearly) not excited when, as in normal operation, only Z_1 is activated. (For details, see [3].) Although the resonance at 1.5 kHz does not affect the scanning, it is detrimental in connection with the coupling in of external vibrations, and in future designs it should be pushed to higher frequencies.

The rough stepping device is a conventional louse system with anodized aluminum feet moving over a stainless-steel plate. In order to maintain a high rigidity and thermal stability, the sample is mounted on one of the feet of the

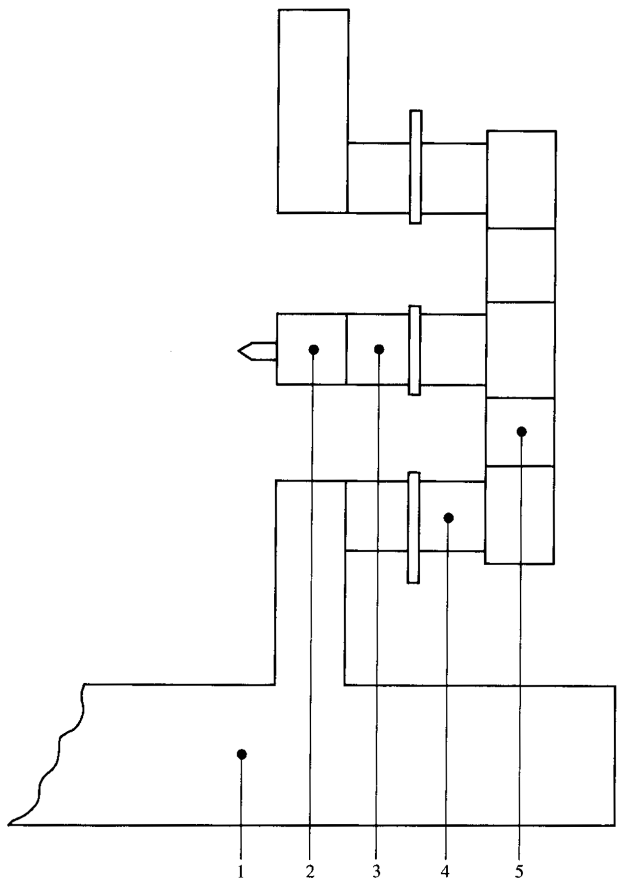

Figure 2

Cross section of the continuous system: (1) Base plate, (2) tip holder with tip, (3) Z_1-piezoelectric system, (4) Z_2-piezoelectric system, (5) x-y-displacement system.

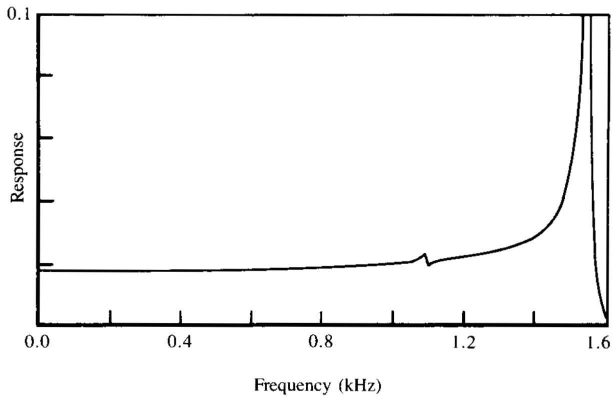

Figure 3

Frequency response of the system while in normal feedback mode. The response is measured by applying a white-noise voltage to the Z_2-piezoelectric system and simultaneously observing the feedback voltage on the Z_1 system.

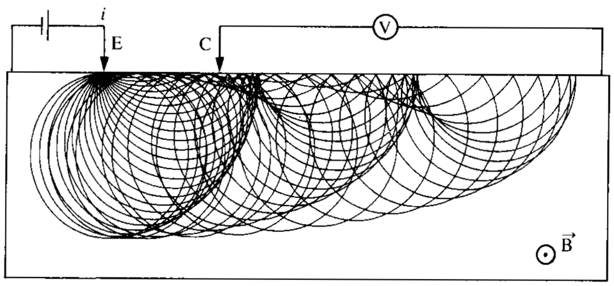

Figure 4

Principle of the transverse electron focusing method. Electrons injected at the emitter E are focused by a magnetic field B at the surface. By sweeping the magnetic field, one or more voltage peaks can be observed at the collector C.

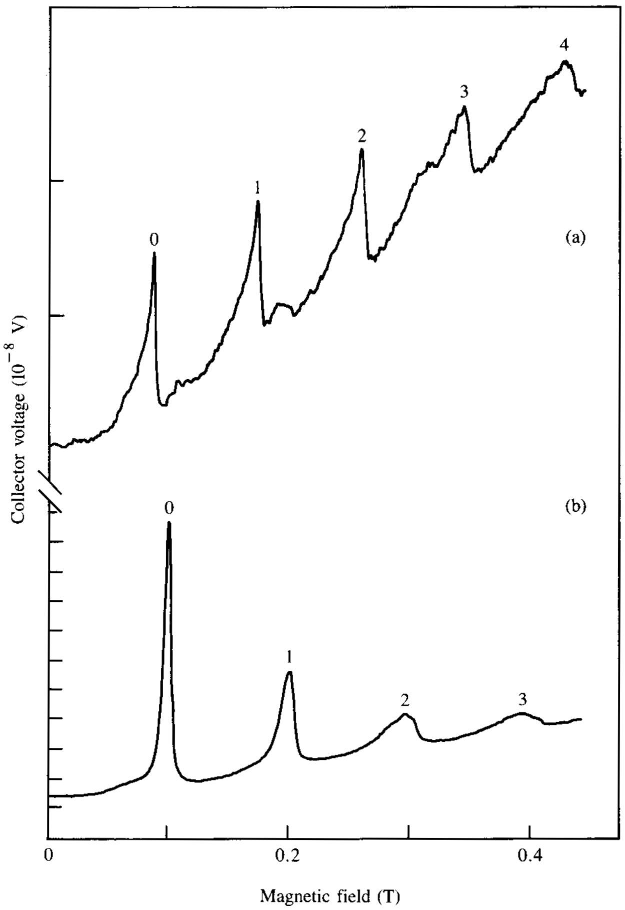

Figure 5

Observed TEF signal versus magnetic field. (a) Ag(001) surface with high specular reflectivity. (b) Ag(011) surface with a quite low specular reflectivity.

louse system. The thermal drift is ≤3 Å/min along the surface and ≤0.5 Å/min perpendicular to the surface.

The vibration-isolation system is quite simple, consisting of a heavy mass hanging on three soft steel springs. Viton links are used for attenuation of acoustic waves propagating in the springs. No active damping has been applied, because frequencies above the resonance frequency are attenuated $\propto 1/\omega^2$ without damping and $\propto 1/\omega$ with damping.

An analysis of the frequency spectrum of the tunnel signal shows building vibrations (18 Hz, 0.04 Å rms) and the resonance of the spring system (3 Hz, 0.08 Å rms). In addition, there is a white-noise contribution with a $1/f$-like tail of unknown origin bringing the total noise level to 0.15 Å rms. No response to acoustic signals was present for normal levels of acoustic energy.

From the response measurements it follows that the response time is smaller than 0.3 ms, so high scanning rates can be used. However, at present the scanning rate is limited by the signal processing to 400 points/s.

2. STM application to a TEF problem

The principle of TEF is explained in **Figure 4**. Electrons are injected by the emitter point contact in a metal single crystal. At a second contact, the collector, under condition of long mean free path, a voltage peak can be observed when a magnetic field focuses the electrons, directly or via specular reflections, on this contact. An example is given in **Figure 5**. The conduction electrons will only be specularly reflected when the surface (seen from the inside) is smooth on a scale of the de Broglie wavelength of the electrons (≃5 Å for Ag). Quite remarkably, high specularities have been observed for a large number of metals and semimetals, both by Tsoi and by our group [2, 4, 5], even for samples which are not polished but only chemically etched and which sometimes

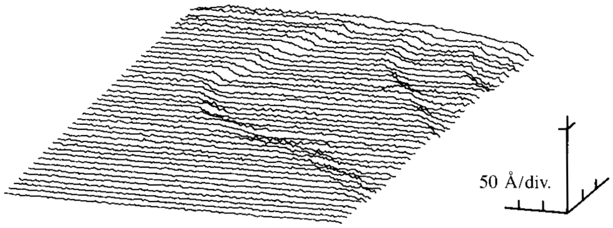

Figure 6

STM observation of a Ag(001) surface. The clearly visible steps have a height corresponding to one unit cell. Note the difference in scale of the horizontal and vertical axes.

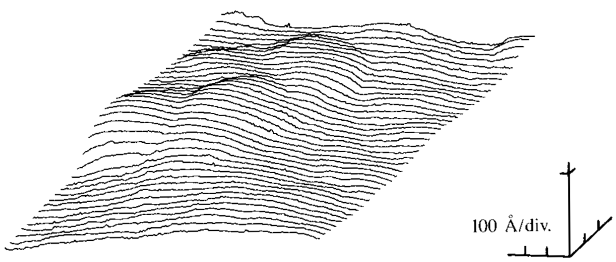

Figure 7

Surface of a Ag(011) crystal.

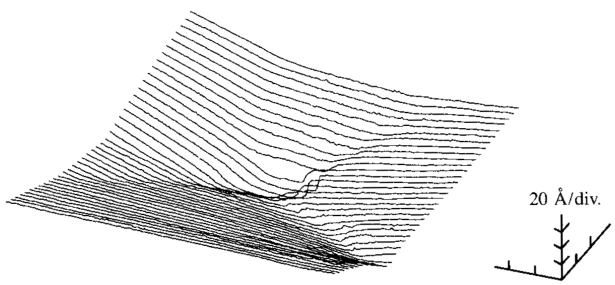

Figure 8

STM measurement of an indentation in a surface made by pushing the tip carefully into a flat part of a Ag(001) surface.

have a rough appearance when viewed with an optical microscope. This apparent discrepancy can be solved by assuming that the surface consists of flat terraces separated by more or less steep slopes such that on a microscopic scale a rough surface is formed. To verify this assumption we compared TEF and STM measurements on (001) and (011) Ag surfaces. The last stage in the surface preparation was an etch in a mixture of H_2O_2 and NH_3 solution. The TEF

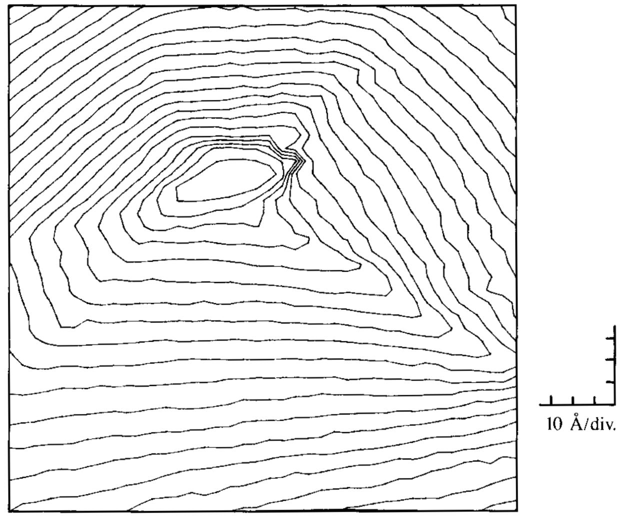

Figure 9

Equal-height-contour-line diagram of the same part of the surface as shown in Figure 8. The lines correspond to height differences of 6.1 Å. The facet structure is clearly visible.

result, averaged over about 100 observations, gave a specularity coefficient $\bar{q}$ of 0.64 for the (001) surface [5]. A typical STM observation is given in **Figure 6**. As shown by this figure and many other observations, the surface consists in large part of atomically flat terraces. From the many STM pictures taken, we can conclude that roughly half of the surface is sufficiently flat to specularly reflect and focus the electrons on the collector. The (011) surfaces showed a lower specularity: $\bar{q} = 0.37$. The STM graphs of the (011) surfaces show surfaces which vary from atomically flat regions via smoothly curved regions to highly corrugated regions (**Figure 7**). In general they had a considerably more hilly appearance than the (001) surfaces.

3. The tip

To interpret the high-resolution STM topographic data it is necessary to know the shape of the tip. In this section, preparation of our tip is described and observations of its shape are presented.

The tip is fabricated from a drawn 0.1-mm-diameter W wire which has its axis in the [011] direction. An electrochemical etch procedure resulted in a tip with a radius of approximately 1 μm. Further preparation involved melting of the tip by applying a large current in shorted position in UHV.

Several methods were used to study the structure of the tip. The most detailed information was obtained by pushing the tip carefully a few hundred Å into a flat part of a silver single-crystal surface and following this with an STM scan of the indented surface. An example is shown in **Figure 8**.

Especially when the result is shown in an equal-height contour diagram, it is clearly visible (**Figure 9**) that the indentation has well-defined faces which extend to about 10 Å from the top. When we consider the hardness of the tungsten tip with respect to the Ag sample, it seems plausible that the indentation represents the shape of the tip to a certain extent. Details of the order of 10 Å around the top will be lost because of the finite tunneling distance. The top angles of the pyramidal tips, taken relative to the axis of the wire, are ≤50°.

Additional information has been obtained by observing the used tip by conventional SEM, TEM, and STEM. **Figure 10** shows clearly the spherical globule caused by tip melting. (This feature is absent in unused tips which underwent an identical etch procedure.)

When studied by STEM and TEM, a rough region visible on the spherical part resolves into an agglomeration of mini-tips approximately 1000 Å wide at the base.

Some topographic STM observations show extremely steep slopes (**Figure 11**, slope 90°, height ≃ 100 Å), which cannot be explained by the described tip shape. Possibly during those measurements the mini-tip carried a whisker-like micro-tip. The present experiment is unable to detect this kind of configuration because the micro-tip probably will be crushed during indenting, and even when it is not crushed the sharp indentation will not be detected by the scan because of the finite tunneling distance. Hence other experiments are needed to solve definitively the origin of the steep slopes.

Figure 10

Scanning electron microscope picture of the tip after prolonged use. In the rough part, visible on the globule, mini-tips with bases of the order of 1000 Å can be seen when viewed at higher magnification.

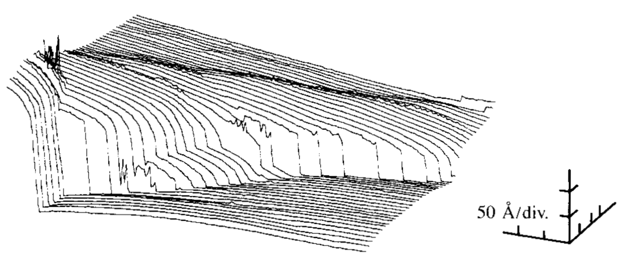

Figure 11

A part of the Ag(001) surface which shows extremely steep slopes.

4. Summary

A description of our STM has been given. During the design special attention was directed towards making the instrument insensitive to vibrations and minimizing the thermal drift, while relatively little attention was paid to vibration isolation. The mechanical characteristics of the STM have been described. The instrument has been used to throw light on a problem in the field of transverse electron focusing, another method of studying surfaces. A description of tip preparation and tip shape has also been presented. It appears that the tip carries pyramidal mini-tips, and in addition there are indications that the tip may sometimes carry whisker-like micro-tips. This last point, however, needs more study.

Acknowledgments

The authors wish to thank Ing. C. J. Beers, Ing. J. W. Gerritsen, and Ing. J. G. Hermsen for their essential contribution to the construction of the STM; Dr. P. A. M. Benistant for his cooperation on the STM-TEF comparison experiment; Ing. A. W. Dicke, Dr. A. L. H. Stols, and Ing. H. T. J. Smits for the electron-microscopic observations; and Prof. Dr. P. Wyder for his stimulating discussions. Part of this work was supported by the Stichting voor Fundamenteel Onderzoek der Materie (FOM), with financial support from the Nederlandse Organisatie voor Zuiver Wetenschappelijk Onderzoek (ZWO).

References

1. G. Binnig and H. Rohrer, *Physica* (Utrecht) **127B**, 37 (1984) and references therein.
2. V. S. Tsoi, *ZhETF Pis. Red.* **199**, 114 (1974) [*JETP Lett.* **19**, 70 (1974)]; V. S. Tsoi and I. I. Razgonov, *Pis'ma ZhETF* **23**, 107 (1976) [*JETP* **23**, 92 (1976)]; V. S. Tsoi and I. I. Razgonov, *Pis'ma ZhETF* **25**, 30 (1977) [*JETP Lett.* **25**, 26 (1977)].
3. G. F. A. van de Walle, J. W. Gerritsen, H. van Kempen, and P. Wyder, *Rev. Sci. Instrum.* **56**, 1573 (1985).
4. P. J. M. W. L. Birker, H. van Kempen, and P. Wyder, *J. Phys.* (Paris) **C6**, 1128 (1978); V. S. Tsoi, J. Bass, P. A. M. Benistant, H. van Kempen, E. L. M. Payens, and P. Wyder, *J. Phys. F: Metal Phys.* **9**, L221 (1979).

5. P. A. M. Benistant, Ph.D. Thesis, University of Nijmegen, Krips Repro, Meppel, The Netherlands, 1984.

Received September 13, 1985; accepted for publication October 30, 1985

Herman van Kempen *Research Institute for Materials, Faculty of Science, University of Nijmegen, Toernooiveld, 6525 ED Nijmegen, The Netherlands.* Dr. van Kempen obtained a Ph.D. degree in low-temperature solid-state physics at the Leiden University, The Netherlands, in 1965. From 1965 to 1967 he was a visiting scientist at Bell Telephone Laboratories, Murray Hill, New Jersey. In 1967 he joined the solid-state physics group of the University of Nijmegen. The academic year 1980–81 was spent as a sabbatical year at the University of California at Berkeley. Dr. van Kempen's current interests include transport properties of pure metals, applications of scanning tunneling microscopy, and transverse electron focusing.

Gerjan F. A. van de Walle *Research Institute for Materials, Faculty of Science, University of Nijmegen, Toernooiveld, 6525 ED Nijmegen, The Netherlands.* Since 1982 Dr. van de Walle has been with the solid-state research group of the University of Nijmegen, working on his Ph.D. subject, scanning tunneling microscopy. Besides being interested in surface science, he is also strongly interested in the science of surfing. Dr. van de Walle's work is financially supported by the Dutch Foundation for Fundamental Research of Matter, FOM.